Applied Mathematical Modelling 36 (2012) 2082–2093

Contents lists available at SciVerse ScienceDirect

Applied Mathematical Modelling

journal homepage: www.elsevier.com/locate/apm

Laminar flamelet modeling of a turbulent $CH_4/H_2/N_2$ jet diffusion flame using artificial neural networks

M.D. Emami *, A. Eshghinejad Fard

Department of Mechanical Engineering, Isfahan University of Technology, 84156-83111 Isfahan, Iran

ARTICLE INFO

Article history:
Received 4 August 2009
Received in revised form 27 July 2011
Accepted 9 August 2011
Available online 18 August 2011

Keywords:
Flamelet model
Artificial neural network
Non-premixed
Differential diffusion
Turbulent flame

ABSTRACT

The laminar flamelet concept is used in the prediction of mean reactive scalars in a non-premixed turbulent $CH_4/H_2/N_2$ flame. First, a databank for temperature and species concentrations is developed from the solutions of counter-flow diffusion flames. The effects of flow field on flamelets are considered by using mixture fraction and scalar dissipation rate. Turbulence–chemistry interactions are taken into account by integrating different quantities based on a presumed probability density function (PDF), to calculate the Favre-averaged values of scalars. Flamelet library is then generated. To interpolate in the generated library, one artificial neural network (ANN) is trained where the mean and variance of mixture fraction and the scalar dissipation rate are used as inputs, and species mean mass fractions and temperature are selected as outputs. The weights and biases of this ANN are implemented in a CFD flow solver code, to estimate mean values of the scalars. Results reveal that ANN yields good predictions and the computational time has decreased as compared to numerical integration for the estimation of mean thermo-chemical variables in the CFD code. Predicted thermo-chemical quantities are close to those from experimental measurements but some discrepancies exist, which are mainly due to the assumption of non-unity Lewis number in the calculations.

1. Introduction

Physical and chemical phenomena in turbulent flames are governed by the continuity, momentum, energy and species transport equations [1]. Direct Numerical Simulation (DNS) of these equations is restricted to simple geometries [2]. The role of the turbulence model and combustion model is to close the averaged governing equations for calculating thermo-chemical scalars in reactive flows without direct resolution of these equations for the species and temperature.

Most of the industrial flames are of a non-premixed type, also referred to as diffusion flames. The simplest combustion model for this type of flame is the flame-sheet model, which has been used for many years to predict the combustion of gaseous fuels [3]. However, this model suffers from several drawbacks [3]. The flamelet model circumvents such limitations and is able to treat the interaction between turbulence and finite rate chemistry. The laminar flamelet model considers complex physical phenomena, such as detailed chemistry and formation of pollutants, by decoupling chemical reactions from turbulent flow field [4]. The flamelet model assumes a turbulent flame as an ensemble of laminar flamelets [4,5]. Each flamelet is subjected to the local flow field conditions, resulting in convection and stretch of the flamelets. Therefore, the local flame structure may be described only by the local flow parameters, especially the local mixture fraction and local scalar dissipation rate corresponding to the stoichiometric mixture. The scalar dissipation rate represents the influence of turbulence on

* Corresponding author. Tel.: +98 3113915245; fax: +98 3113912628.
E-mail address: mohsen@cc.iut.ac.ir (M.D. Emami).

0307-904X/$ - see front matter © 2011 Elsevier Inc. All rights reserved.
doi:10.1016/j.apm.2011.08.012

flamelet structure and can be interpreted as the inverse of characteristic diffusion time [4]. The laminar flamelet structure can be pre-calculated and tabulated into a flamelet library, with mixture fraction and scalar dissipation rate as independent variables. Once the values of these parameters are known from the flow field, one can find thermo-chemical quantities from the flamelet library [6].

Flamelet formulation for turbulent non-premixed flames was first presented by Peters [4] in 1984, who used probability density function to obtain the mean reactive scalars. Further developments of this model made it quite popular among the combustion researchers. The model has been successfully applied to predict flow variables in many applications, both for turbulent and laminar flames [7–13]. Sanders et al. [8] explored the laminar flamelet model for predictions of NOx emissions from turbulent hydrogen jet diffusion flames. The flamelet model gives better predictions when the Damköhler number increases, corresponding to thin flames in which the smallest turbulent eddies are still bigger than the flame thickness. Coelho and Peters [9] applied the Eulerian particle flamelet model (EPFM) to calculate the NOx formation in a combustor with high preheating and strong internal exhaust gas recirculation. Claramunt et al. [1,11] investigated the application of the laminar flamelet numerical simulation of multidimensional non-premixed laminar flames comparing different flamelet mathematical formulations. Unsteady flamelet model is used to account for slow processes like pollutant formation, as the chemical flamelet structure can then follow rapid changes of the scalar dissipation rate instantaneously. Lee and Choi [13] applied unsteady flamelet model to the combustion and pollutant emissions of turbulent jet flames of methane and propane with various conditions of inlet air temperature and oxygen concentration. Their results revealed that, when the oxygen concentration is high, the two fuels show quite different characteristics in the downstream region. Furthermore, propane gives a higher NO formation compared to methane, especially when the oxygen concentration is high.

One of the main goals of this paper is to apply artificial neural networks (ANNs) to model non-premixed turbulent flames. ANNs are promising modeling techniques that have very good approximation capabilities. The first studies concerning ANNs can be traced back to 1940s, but their applications were limited until 1980s. Presentation of the Error Back Propagation (EBP) algorithm, by Rumelhart et al. [14], resulted in their widespread use in practical applications such as aerospace, banking, automotive industry, transportation, signal processing, insurance, automatic control and many other fields. Their use is expected to increase due to developments in computational methods in the coming decade [15]. The applications of ANN to combustion problems have been reported in few previous works [16–21]. The present paper is an effort to develop the ANN–flamelet technique for RANS simulation of DLR flame.

Kempf et al. [19] investigated the structure of a diffusion flame by using Large Eddy Simulation (LES). A steady flamelet model, which is represented by an artificial neural network, yields flow field parameters as a function of the mixture fraction. They assessed the accuracy of the results by varying the grid-resolution and by comparing to experimental data. Their results obtained for both one- and two-point statistics were in good agreement with the experimental data.

Sen and Menon [21] evaluated the applicability of ANN approach as a chemistry integrator for LES of turbulent flame. An ANN code based on back-propagation algorithm was developed with a new approach for self-determining the model coefficients adaptively with respect to the error surface topology. They found that once the ANN is well trained, it can successfully predict the reaction rates in both memory and time efficient manner compared to traditional look-up table approach and stiff ODE solvers, respectively.

Ihme et al. [20] performed LES of a bluff-body, methane–hydrogen flame, using two chemistry representation methods, namely a conventional structured tabulation technique and ANN. The method for the generation of optimal artificial neural networks (OANNs) [22] was employed in the LES of turbulent reactive flows. The network performance was compared with the structured tabulation of increasing resolution, and effects of long-time error accumulation on the statistical results during a numerical simulation were discussed.

The work described in this paper concerns the use of steady flamelet modeling approach in calculations of a turbulent $CH_4/H_2/N_2$ jet diffusion flame. Differential diffusion effects have been considered in this study. Mean reactive scalars are calculated using a presumed probability density function. In order to apply the flamelet model to an in-house CFD code, ANN is used. Results are compared to those obtained by measurements and numerical simulations. The effects of non-unity Lewis number assumption and the advantages of ANN in reducing numerical effort and computational time are discussed.

2. The laminar flamelet model

In diffusion flames, combustion occurs in a thin layer in the vicinity of the surface of the stoichiometric mixture, if the local mixture fraction gradient is assumed to be high enough. This thin layer and the surrounding non-reacting mixing region are defined as an ensemble of laminar diffusion flamelets [6].

Using Crocco-type transformation and neglecting the multidimensional effects (convection and diffusion), as well as the derivatives of reactive scalars in tangential direction compared to those in normal direction, flamelet equations for species and temperature can be derived from the conservation equations in the Eulerian framework [1,6]:

$$\rho \frac{\partial Y_i}{\partial t} = \frac{\rho}{Le_i} \frac{\chi}{2} \frac{\partial^2 Y_i}{\partial Z^2} + \dot{\omega}_i, \tag{1}$$

$$\rho\frac{\partial T}{\partial t}=\frac{\rho}{Le_i}\frac{\chi}{2}\frac{\partial^2 T}{\partial Z^2}-\frac{1}{c_p}\sum_{i=1}^{N}h_i\dot{\omega}_i+\frac{Q_R}{c_p}, \tag{2}$$

where Y_i is mass fraction of species i, T is the temperature, and Z is the mixture fraction, which accounts for fuel and oxidizer mixing level. Here $\dot{\omega}_i$ is the chemical production rate of species i, h_i is species enthalpy and Q_R is the radiation heat loss. Parameter c_p denotes the constant pressure specific heat capacity, ρ is the mass density, Le_i is the Lewis number of species i, and χ is the scalar dissipation rate. Omitting the time derivative in the flamelet equations leads to the governing equations of *steady flamelets*.

The scalar dissipation rate can be interpreted as the inverse of a characteristic diffusion time. As this time decreases, mass and heat transfer through the stoichiometric plane are enhanced. The scalar dissipation rate is defined by:

$$\chi=2D|\nabla Z|^2, \tag{3}$$

where D is the diffusion coefficient. At the flame surface, the scalar dissipation rate is given by the stoichiometric value, χ_{st}, which can be modeled by the following expression for a counter-flow diffusion flame with a small stoichiometric mixture fraction:

$$\chi_{st}=\frac{a(j+1)}{\pi}\exp(-2[erfc^{-1}(2Z_{st})]^2). \tag{4}$$

In Eq. (4), $erfc^{-1}$ is the inverse of complementary error function, and subscript st denotes the stoichiometric condition. Here $j = 0$ and $j = 1$ are used for the planar and axially symmetric configurations, respectively. Thus, χ_{st} is proportional to the strain rate, a, for a counter-flow diffusion flame.

There are commonly two ways to apply the steady flamelet concept to modeling a diffusion flame. One method is to solve the steady state form of Eqs. (1) and (2) in the mixture fraction coordinate with properly defined boundary conditions and a specified characteristic scalar dissipation rate. The second one, which is adopted in the present work, is to solve the governing equations of counter-flow diffusion flame along the stagnation streamline (physical space) with an arbitrarily complex chemistry for different values of χ_{st}. A range of χ_{st} can be obtained by varying the strain rate parameter a in the counterflow laminar flame calculations (Eq. (4)). The mixture fraction is calculated from the products mass fractions using the method of Bilger et al. [23]:

$$Z=\frac{2(Y_C-Y_{C,2})/w_C+(Y_H-Y_{H,2})/2w_H-(Y_O-Y_{O,2})/w_O}{2(Y_{C,1}-Y_{C,2})/w_C+(Y_{H,1}-Y_{H,2})/2w_H-(Y_{O,1}-Y_{O,2})/w_O}, \tag{5}$$

where Y's are elemental mass fractions of carbon, hydrogen and oxygen; w's are atomic weights; and the subscripts 1 and 2 refer to the fuel and air streams, respectively.

Species mass fractions and temperature are functions of the mixture fraction and stoichiometric scalar dissipation rate:

$$Y_i=Y_i(Z,\chi_{st});\quad T=T(Z,\chi_{st}). \tag{6}$$

The influence of turbulent fluctuations on the thermo-chemical quantities may be taken into account by using presumed probability density functions. The Favre mean and the variance of a thermo-chemical scalar can then be obtained from the following relations [24]:

$$\tilde{\varphi}(\tilde{Z},\widetilde{Z''^2},\widetilde{\chi_{st}})=\int_0^1\varphi(Z,\chi_{st})P(Z)dZ, \tag{7}$$

$$\widetilde{\varphi''^2}(\tilde{Z},\widetilde{Z''^2},\widetilde{\chi_{st}})=\int_0^1(\varphi(Z,\chi_{st})-\tilde{\varphi})^2P(Z)dZ, \tag{8}$$

where $\tilde{Z}$ and $\widetilde{Z''^2}$ are the mean and variance of mixture fraction, respectively. Variables with over-tilde denote density weighted (Favre) mean quantities, and $P(Z)$ is a presumed pdf, usually the incomplete β-function that only depends on the mean and variance of mixture fraction.

The Favre mean species concentrations and temperature are stored in the flamelet library. Thus, if the local values of $\tilde{Z}$, $\widetilde{Z''^2}$ and $\widetilde{\chi_{st}}$ are known, the mean species concentrations and temperature can be determined from the flamelet library. Values of the mean and variance of mixture fraction are calculated at each grid point of domain by solving their transport equations, and the mean scalar dissipation rate is modeled as:

$$\widetilde{\chi_{st}}=\frac{\tilde{\chi}f(Z_{st})}{\int_0^1 f(Z)P(Z)dZ}, \tag{9}$$

$$f(Z)=\exp(-2[erfc^{-1}(2Z)]^2), \tag{10}$$

where the mean value $\tilde{\chi}$ may be modeled by the values of turbulent kinetic energy $\tilde{k}$, its dissipation $\tilde{\varepsilon}$ and mixture fraction variance [6]:

$$\tilde{\chi} = c_\chi \frac{\tilde{\varepsilon}}{\tilde{k}} \widetilde{Z''^2}, \tag{11}$$

where $c_\chi = 2$ has been widely used in the literature [6].

3. Artificial neural networks (ANN)

ANNs are collections of some processing units and act as a black box that learns the relation between inputs and outputs. A neural network consists of a large number of computing elements, called neurons, which are tied together with weighted connections and are arranged in layers. Each neuron comprises one or more inputs, weight and a transfer function. The role of each neuron is to receive the input, add the weighted input to bias and calculate the output by applying a transfer function on it. The transfer function may be linear, sigmoid, etc. [25,26].

ANNs are often classified according to the number of layers, single or multi layer. Multi layer ANNs contain hidden layers between the input and the output. The capability of multi layer networks is higher than single layer ones. For example, a two layer network with sigmoid transfer function in the first layer and a linear transfer function in the second layer is able to approximate most functions [25], which is also employed in this study.

Feedforward ANNs are those networks in which there is no feedback of the output signals. A two-layer feed forward network architecture is shown in Fig. 1, where R is the number of inputs, S^1 and S^2 are the number of neurons in the first and second layer, respectively. Parameter b is the bias, w is the weight and a is the output. Subscripts are used to identify the neurons and superscripts to identify the layers.

An important stage for an ANN is the training step, in which the input is fed to the network and its output is generated. Comparing the calculated and desired outputs, network attempts to adjust its parameters in order to minimize the error between target and actual output. Network training is usually implemented for function approximation (nonlinear regression), pattern association and pattern classification. Multi Layer Perceptron (MLP) networks are extensively used for these purposes and are often trained by EBP algorithm where the input is forward propagated through layers to an output layer. After an error between the output and the desired value is determined, it is back-propagated through the network connections from the output to the input layer for adjusting weighting values. This process of network training is repeated until all the weights have stabilized and the error has reached an acceptable level.

In the present study, MLP networks with two layers (in addition to input layer) are used. Determination of the optimum number of neurons in hidden layers is carried out by a trial and error procedure.

4. The research approach

Steady state, counter-flow diffusion flame calculations are performed, using the OPPDIF computer code [27]. The chemical mechanism considered is GRI-Mech 3.0 [28], involving 53 species and 325 reactions. Mixture fraction is calculated using Bilger's formula [23] and scalar dissipation rate is considered proportional to the strain rate.

In order to obtain mass fractions and temperature (as a function of mixture fraction and scalar dissipation rate) a neural network (ANN1) is created. Mixture fraction and scalar dissipation rate are selected as inputs and species mass fractions and temperature, which is normalized by its maximum value, are defined as outputs. Then, this network (ANN1) is used to estimate φ_i for the calculations of Favre mean scalars by Eq. (7). Numerical integration is performed over the range of mean and variance of mixture fraction and scalar dissipation rate to create a databank. It must be noted that this integration is carried out by the procedure suggested in [29] and by considering more integration points near extremes and around the

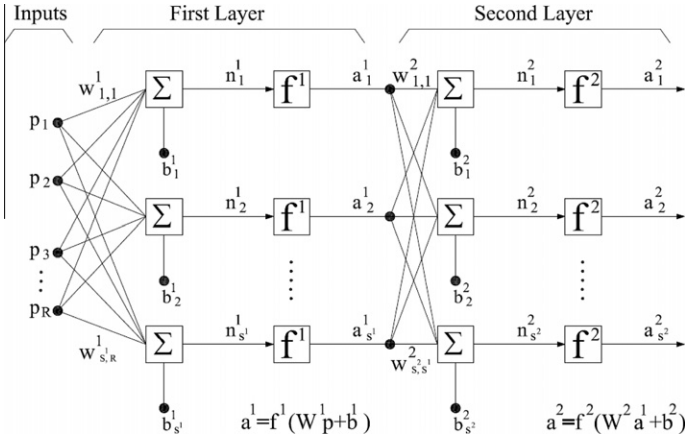

Fig. 1. Architecture of a two layer feed forward neural network.

stoichiometric value. In the next step, another network (ANN2) is developed over the generated databank, where the three aforementioned parameters (mean and variance of mixture fraction and scalar dissipation rate) are employed as inputs and the *mean* values of species mass fractions and normalized temperature are selected as outputs. Finally, weights and biases of this network (ANN2) are implemented in the CFD code to predict the mean reactive scalars during an iterative computational procedure.

In the case of network training, the Levenberg–Marquardt algorithm [25] is used to optimize the synaptic weights. This algorithm is a robust Gauss-Newton method and its fast convergence makes its suitable for training neural networks. A two-layer architecture was found adequate for the prediction of species mass fractions and temperature, as recommended by Hagan et al. [25]. The final network (ANN2) has 8 neurons in the first layer (hidden layer) and 11 neurons in the second layer (output layer) and is able to predict the Favre mean temperature and mass fractions of the main species, as well as minor species. Typically, the training set used for the adjustment of parameters of ANN2 has 4550 sets of data, and around 1500 additional sets are used for the test step. The network outputs and target values were almost identical and there were not appreciable differences between them.

The numerical simulation software is an in-house computer code, based on the finite volume discretization method on structured, collocated cells. The method is second order accurate regarding convection, diffusion and source term discretization. In addition to the basic equations for the flow field, equations for the mean mixture fraction and its variance are solved in the present code using the standard k–ε model, to deal with turbulence [30]. The standard k–ε model has known shortcomings for predicting round jets. In particular, the k–ε model over-predicts the decay rate and the spreading rate of a round jet. In the present work, a simple modification to the value of $C_{\varepsilon 1}$ of the ε-transport equation is made. The value of constant $C_{\varepsilon 1}$ is modified from 1.44 to 1.60 following the work of McGuirk and Rodi [31]. The SIMPLEC algorithm is used to handle pressure and velocity coupling. It is noteworthy that the validity of this code has been verified in previous studies [32].

In the present work, by adding proper sub-routines, mean values of the thermo-chemical parameters and temperature are obtained for each grid node in the calculation domain and results are compared with experimental measurements, unsteady flamelet calculations, and equilibrium model predictions.

4.1. The test case

The flame modeled here is a turbulent $CH_4/H_2/N_2$ jet diffusion flame, known as DLR-A flame, which has been experimentally investigated by Bergmann et al. [33] and Hassel and Geiß [34]. The fuel has a composition of 22.1% CH_4, 33.2% H_2 and 44.7% N_2 in volumetric parts, issuing from a stainless steel tube with an inner diameter of 8 mm at velocity of 42.2 ± 0.5 m/s (Re = 15,200).

Hydrogen is used in the experiments to stabilize the flame and nitrogen is added to decrease thermal radiation and to improve the quality of measuring techniques. Coflow air enters the flow field via an annular nozzle (140 mm diameter) with an exit velocity of 0.3 m/s. Fuel and air temperatures are both 295 K. The system works in atmospheric pressure and the stoichiometric mixture fraction is 0.167. Experimental data has been gathered by means of Raman–Rayleigh, LIF measurements [35,36]. Conditional Moment Closure and unsteady flamelet results are given in [37,38], respectively. In the present work, the experimental data for the Favre mean temperature and mass fractions are obtained from the website of Sandia National Laboratories [35].

An axisymmetric computational domain with 1.5 m length and 15 cm radius has been considered to isolate the effects of walls on the flame structure, based on the available experimental data. In the present case, grid independent solutions were established by using 63 nodes in radial direction and 300 nodes in axial direction. Dirichlet and outflow boundary conditions were applied for the inlet and outlet flows, respectively. The no-slip boundary condition was used for solid walls and zero normal gradient condition was imposed at the symmetry axis.

5. Results and discussion

The efficiency of ANN in the numerical procedure is considered first. Computational time for the laminar flamelet modeling of DLR flame has been monitored using two methods. The first is the numerical integration of Eq. (7) in the CFD code at each step of iterations to achieve mean thermo-chemical scalars. The second is to implement the steady flamelet model via ANN; where numerical integration is performed prior to the execution of the CFD code and a neural network is constructed over the library yielding mean thermo-chemical scalars.

A comparison of the CPU performance on a 2.66 GHz Pentium IV personal computer confirms that the ANN method is superior to the direct integration (DI) in the flow solver code. The CPU time for 6 iterations was 79 s when DI was accomplished in the main code, whereas the ANN-based approach took 20 s for 38 iterations. Note that the aforementioned CPU time does not include the time spent on network training. Considering the training time does not violate the superiority of the ANN-based approach, because of its significant amount of memory and time saving during the execution of the CFD code. In addition, the computational time for the training procedure is found to be of minor importance when the grid network is dense, or the number of iterations is notable. An overall reduction factor of 25 has been monitored during several

numerical experiments, when ANN is used. This demonstrates that the ANN method clearly has the potential to be used effectively in the turbulent combustion calculations.

Results of the simulation at three axial locations including $x/D = 5$, 20, 40 ($D = 8$ mm), where x is the axial distance from the burner, are shown in Figs. 2–6. In these figures, the results of the steady laminar flamelet model with $Le \neq 1$ are referred to as "Flamelet + ANN" model. The experimental data and the unsteady flamelet results (with $Le = 1$) of Pitsch [38], which are published for few species and stations, are also shown in these figures (computational results of [38] were not available for $x/D = 20$). Simulations were also carried out for the "equilibrium" approach.

Since the focus of the present study was on the evaluation of the ANN-based flamelet model, turbulent flow field predictions were optimized based on mixture fraction data. This involves a slight adjustment of the $C_{\varepsilon 1}$ constant, to obtain the best fit against radial data profiles, with values of $C_{\varepsilon 1}$ falling between the standard value and the revised value of 1.6. Furthermore, the errors caused by the wrongly predicted radial mixture fraction profile are minimized by presenting the radial data of quantities as a function of the mean mixture fraction.

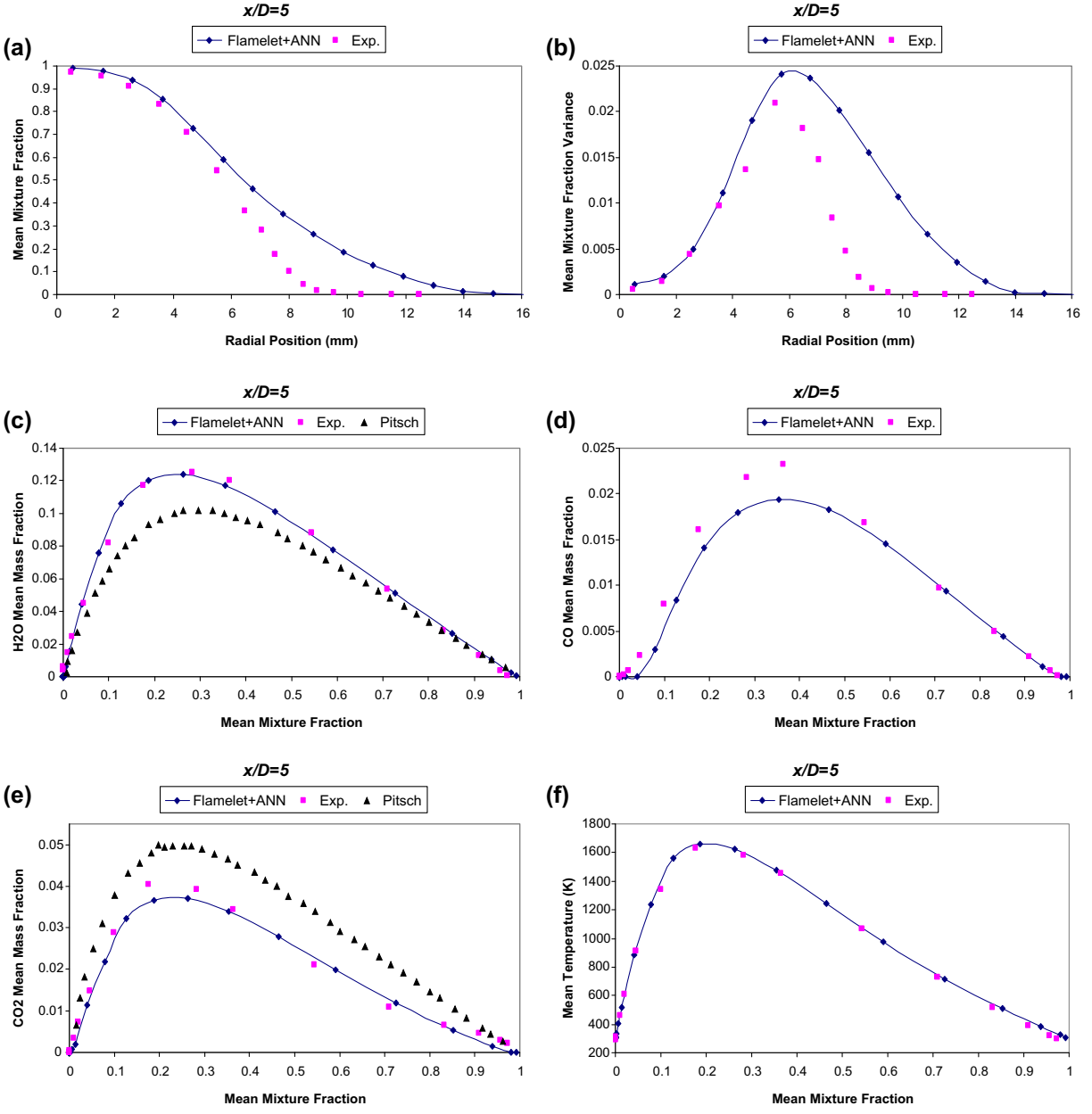

Fig. 2. Radial distributions of mean and variance of mixture fraction and profiles of Favre mean mass fractions of H_2O, CO, CO_2 and temperature vs. mean mixture fraction at $x/D = 5$.

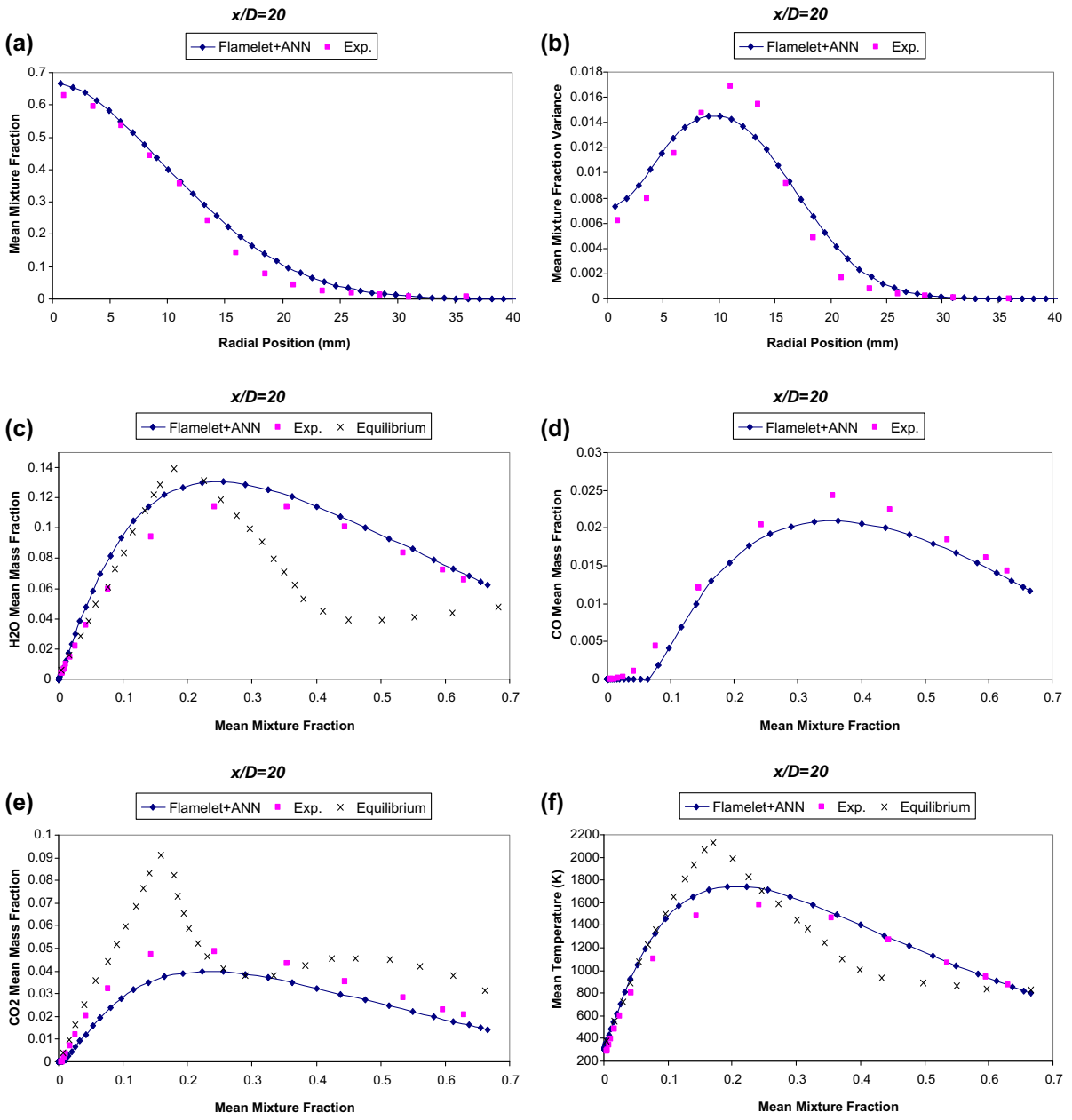

Fig. 3. Radial distributions of mean and variance of mixture fraction and profiles of Favre mean mass fractions of H_2O, CO, CO_2 and temperature vs. mean mixture fraction at $x/D = 20$.

Fig. 2a and b depict, respectively, the results for radial distributions of mean mixture fraction and its variance close to the nozzle exit at $x/D = 5$. One can see in Fig. 2a that there is over-prediction of mean mixture fraction in the region $r > 5$ mm. The values of mixture fraction variances in Fig. 2b are also over-predicted by k–ε model for this region. The above feature of the mixture fraction and its variance in the first section reveals an over-estimation of mixing when two-equation turbulent models are applied. This is in accordance with the observations of Tabet et al. [39] for this flame. They stated that modeling of turbulence in regions with strong density gradients in the turbulent flow field at high velocities could cause the differences and improvement of mixing is achieved by using the LES approach.

The H_2O profile for the "Flamelet + ANN" model (see Fig. 2c) matches the experimental data, but the results of Pitsch under-predict the H_2O mass fraction, which is mainly due to neglecting the differential diffusion effects, and will be discussed later.

It is seen in Fig. 2d that CO profile in the steady state flamelet model is slightly under-predicted. As the formation of CO is slow relative to other species in the radical pool, the steady state model is in fact expected to yield poor agreement.

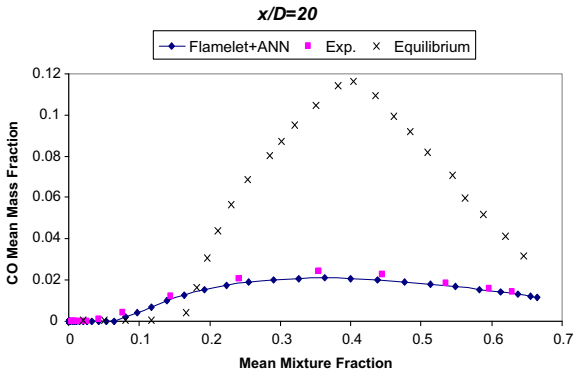

Fig. 4. Favre mean mass fraction of CO at $x/D = 20$.

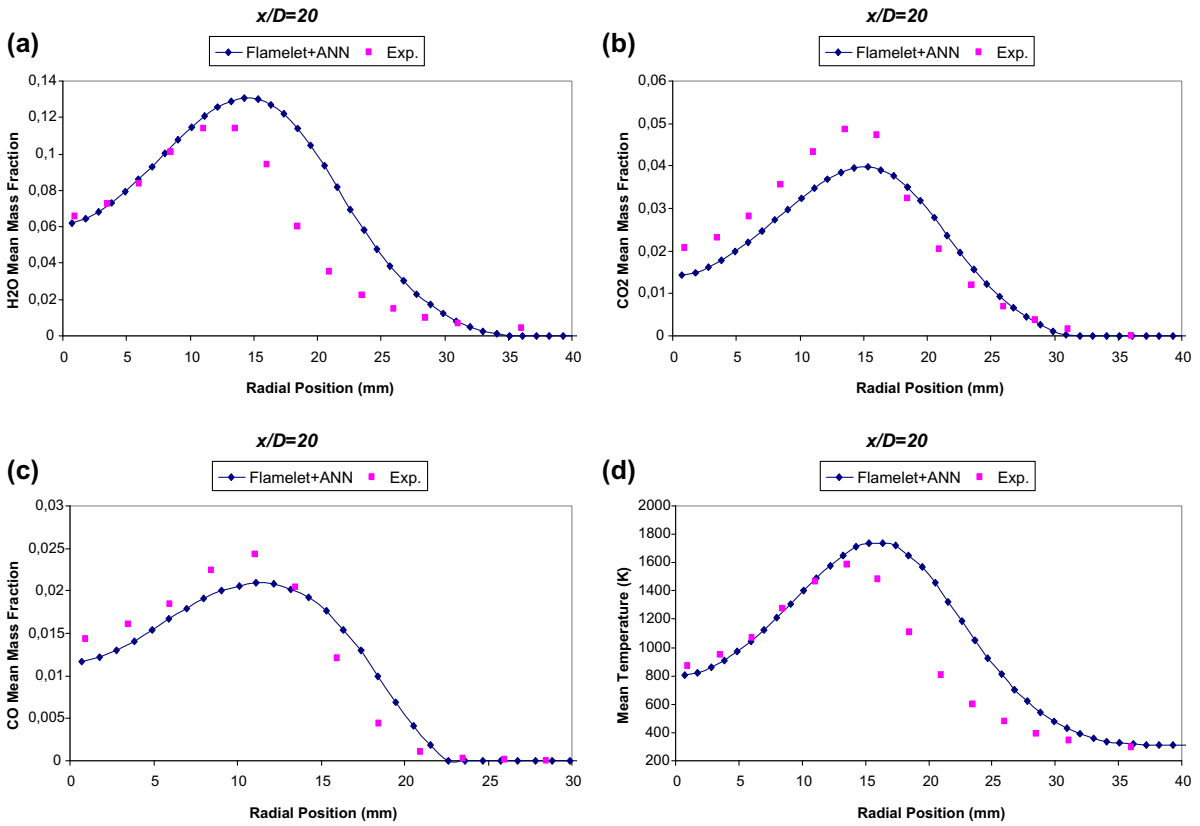

Fig. 5. Radial distributions of Favre mean mass fractions of H_2O, CO, CO_2 and temperature at $x/D = 20$.

The assumption of unity Lewis number in the unsteady flamelet model results in higher CO_2 level predictions of [38] in Fig. 2e, whereas the result of the present steady flamelet model (with $Le \neq 1$) has better agreement with the data. This can be attributed to the differential diffusion effects. In the region close to burner exit, the increase of kinematic viscosity, due to heat release, leads to the laminarization of the turbulent field [36]. Therefore, calculations for CO_2 mass fractions with $Le \neq 1$ assumption are more justified in comparison to $Le = 1$, both in the fuel-lean and fuel-rich sides. It is interesting to mention that the transition from laminar-like to turbulent-like region occurs beyond $x/D = 5$, according to [36].

The temperature profile for the "Flamelet + ANN" approach at $x/D = 5$ (see Fig. 2f) shows very good agreement with the measured one, mostly due to taking account of the differential diffusion in the flamelet library.

Measured and predicted Favre mean mass fractions and temperatures at $x/D = 20$ are compared in Fig. 3. The predicted values of the mean and variance of mixture fraction in this station demonstrate good agreement with experimental data.

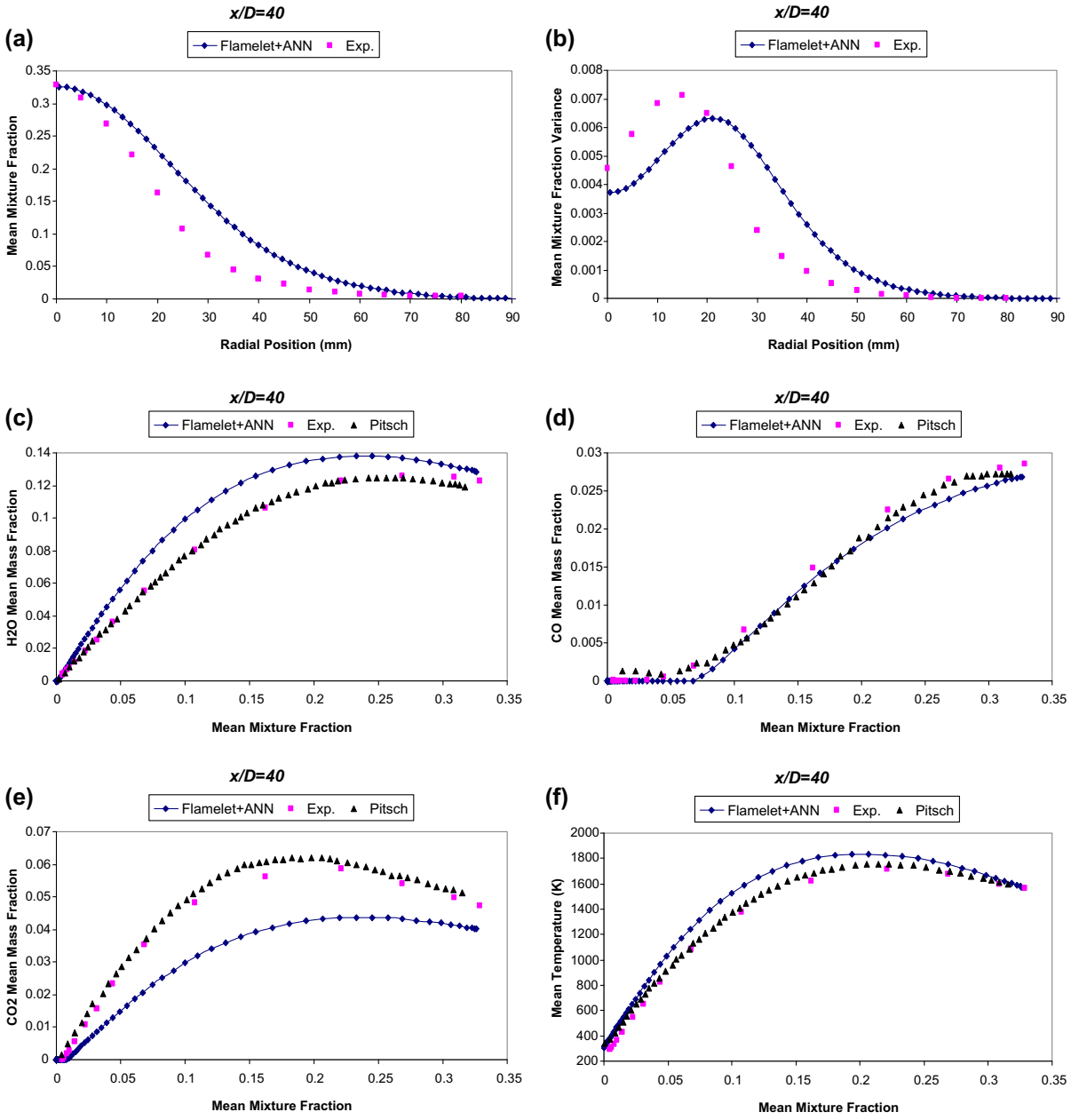

Fig. 6. Radial distributions of mean and variance of mixture fraction and profiles of Favre mean mass fractions of H_2O, CO, CO_2 and temperature vs. mean mixture fraction at $x/D = 40$.

It is observed that the equilibrium profiles (Fig. 3c, e and f), which are obtained from CHEMKIN II code [40], deviate substantially from measurements since it assumes thermal decomposition of methane to take longer than is usually anticipated in turbulent jet flames, as explained by Meier et al. [36].

Steady flamelet profiles for species mass fractions are in reasonably good agreement with measurements, although the difference between the calculated and experimental data is larger, when compared to $x/D = 5$. This deviation is not surprising, because contrary to what observed in the former location ($x/D = 5$), the flow regime at $x/D = 20$ is completely turbulent and the rate of transport phenomena is governed by turbulent diffusion. It also causes the rate of diffusion of heat and mass to be similar, and therefore the assumption of $Le \neq 1$ leads to poorer results, especially for CO_2 concentration.

The temperature profile is over-estimated by the Flamelet + ANN approach (Fig. 3f) due to the strong influence of differential diffusion. The equilibrium model gives higher values at the stoichiometric region associated to the adiabatic temperature ($T_{ad} = 2130$ K).

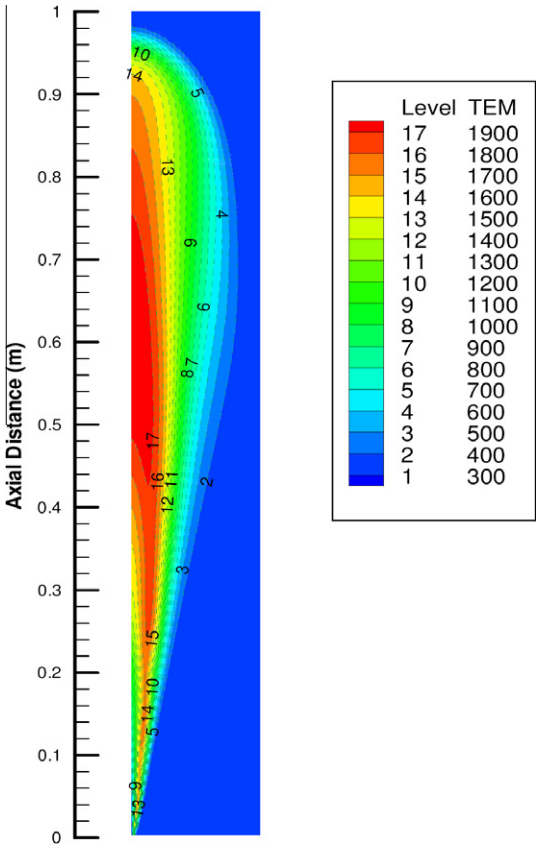

Fig. 7. Computed contours of mean temperature (K).

Fig. 4 presents CO profile obtained from equilibrium approach compared to experiments and flamelet results at $x/D = 20$. The equilibrium model extremely over-predicts CO level in the $Z > Z_{st}$ region. A possible reason for the behavior is that the diffusion time in the turbulent flame is not enough to establish an equilibrium solution. However, it is expected that getting further downstream of the burner, as the strain rate decreases, the equilibrium condition prevails.

Fig. 5 represents the measured and calculated radial profiles of thermo-chemical quantities at $x/D = 20$. It may be inferred from Fig. 5a and d that the over-estimation of H_2O level in the fuel-lean region is closely tied to the over-estimation of temperature and both profiles follow the same trend, and is consistent with errors in the mean mixture fraction variance at this station. The deviations between the calculations and the measurements for different species are mainly attributed to the deficiencies of the turbulence model and differential diffusion. Using Reynolds stress turbulence model can lead to better predictions of radial profiles [37].

Measured and predicted Favre-averaged species mass fractions and temperature at $x/D = 40$ are given in Fig. 6. It can be seen that the results of the unity Lewis number calculations are in better agreement with measurements, which confirm that differential diffusion is an important factor in influencing the predictions.

Temperature contours are depicted in Fig. 7 to visualize the development of flame inside the domain. It is seen that a high temperature region is formed around the mixing region, where the stoichiometric mixture fraction is expected, and is transported to downstream. The temperature pattern is consistent with the typical spreading of a jet in a confined environment.

6. Conclusions

The present paper investigates the performance of the steady laminar flamelet model for a turbulent reacting jet. ANNs are used to avoid numerical integration for the calculation of mean thermo-chemical quantities in the CFD code. The use of ANN reduces the computational time and a reduction factor of 25 has been monitored during the execution of the CFD code.

Two-layer networks with sigmoid transfer functions in the hidden layer and linear transfer functions in the output layer have very good computational capabilities for the prediction of major species and temperature. The ANN–flamelet approach can be extended to predict minor species profiles like NO and OH by using more hidden layers and optimizing the networks.

In terms of the turbulent mixing field, including the mixture fraction and its variance, there exist deviations between prediction and measurement. These discrepancies are mainly caused by deficiencies in the k–ε turbulence model. The effect of

non-unity Lewis number has also been studied. It was shown that non-unity *Le* number assumption leads to good results where the laminarization effects are strong, which in the present case occurs only near the inlet nozzle. At downstream locations, *Le* = 1 assumption gives better results (especially for CO_2 mass fraction), as turbulent transport becomes dominant at these locations. Therefore, non-unity Lewis number assumption is the main cause of discrepancy between species profiles predicted by Flamelet + ANN model and those in experimental data for downstream locations.

Comparing the present work and the published paper by Ihme et al. [20], following conclusions can be drawn:

1. The work by Ihme et al. [20] has been devoted to LES of reactive flows, whereas this work applies ANNs to RANS simulation of non-premixed flames. Therefore, they used one ANN for each quantity, while just one ANN is trained here for the prediction of all species concentrations and temperature, which results in a lower training time spent. In addition, the networks of the present work have fewer hidden layers because RANS calculations are typically less sensitive than LES calculations, where unsteady flow fields are evaluated and a much higher accuracy is required to represent a larger region of the composition space accurately. Both papers utilize Levenberg–Marquardt learning algorithm.
2. Ihme et al. [20] stored all filtered thermo-chemical quantities in a structured table as a function of three scalars (mean mixture fraction, unmixedness and a reaction progress variable) and assessed the performance of the table in comparison with optimal networks. They compared data retrieval time from the table and the ANN, contrary to this work where the time spent for the calculation of mean reactive scalars via ANN is compared against direct integration in CFD code. If we only compare table and ANN retrieval, tables are slightly more effective because interpolation in a structured table can be more efficient than computational propagation of information through a connected network and associated evaluation of the transfer functions.

Comparison of the steady flamelet model results and those from the unsteady flamelet approach demonstrates that the steady flamelet concept is adequate for most flames without quenching/extinction effects or when slow processes are insignificant.

The results and discussions lead one to conclude that a combination of optimal neural networks and unsteady flamelet model would be a good choice for simulating most flames with a good level of accuracy.

Acknowledgments

The authors would like to thank Matthias Ihme and Kilian Claramunt for their helpful advice and discussion during the preparation of the paper.

References

[1] K. Claramunt, R. Cònsul, D. Carbonell, C.D. Pérez-Segarra, Analysis of the laminar flamelet concept for nonpremixed laminar flames, Combust. Flame 145 (2006) 845–862.
[2] J.M. Burgerscentrum, Course on Combustion, Eindhoven University of Technology, 2005. Available at: <http://www.combustion.tue.nl/course/lecturenotes.pdf>.
[3] S.P. Burke, T.E. Schumann, Diffusion flames, Ind. Eng. Chem. 20 (1928) 998–1004.
[4] N. Peters, Laminar diffusion flamelet models in non-premixed turbulent combustion, Prog. Energy Combust. Sci. 10 (1984) 319–339.
[5] N. Peters, Laminar flamelet concepts in turbulent combustion, in: 21st Symposium (International) on Combustion, The Combustion Institute, Pittsburgh, 1986, pp. 1231–1250.
[6] N. Peters, Turbulent Combustion, Cambridge University Press, Cambridge, UK, 2000.
[7] D. Lentini, I.K. Puri, Stretched laminar flamelet modeling of turbulent chloromethane-air nonpremixed jet flames, Combust. Flame 103 (1995) 328–338.
[8] J.P.H. Sanders, J.-Y. Chen, I. Gökalp, Flamelet based modeling of NO formation in turbulent hydrogen jet diffusion flames, Combust. Flame 111 (1997) 1–15.
[9] P.J. Coelho, N. Peters, Unsteady modelling of a piloted methane/air jet flame based on the Eulerian particle flamelet model, Combust. Flame 124 (2001) 444–465.
[10] Z. Wen, S. Yun, M.J. Thomson, M.F. Lightstone, Modeling soot formation in turbulent kerosene/air jet diffusion flames, Combust. Flame 135 (2003) 323–340.
[11] K. Claramunt, Numerical Simulation of Non-premixed Laminar and Turbulent Flames by Means of Flamelet Modelling Approaches, PhD Thesis, Universitat Politècnica de Catalunya, Spain, 2005.
[12] A. Odedra, W. Malalasekera, Eulerian particle flamelet modeling of a bluff-body CH_4 /H_2 flame, Combust. Flame 151 (2007) 512–531.
[13] K.W. Lee, D.H. Choi, Analysis of NO formation in high temperature diluted air combustion in a coaxial jet flame using an unsteady flamelet model, Int. J. Heat Mass Transfer 52 (2009) 1412–1420.
[14] D.E. Rumelhart, G.E. Hinton, R.J. Williams, Learning internal representations by error propagation, in: D.E. Rumelhart, J.L. McClelland (Eds.), Parallel Data Processing, The MIT Press, Cambridge, 1986.
[15] L.I. Perlovsky, Multiple sensor fusion and neural networks, DARPA Neural Network Study, MIT/Lincoln Lab, Lexington, MA, 1987.
[16] F.C. Christo, A.R. Masri, E.M. Nebot, S.B. Pope, An integrated PDF/neural network approach for simulating turbulent reacting systems, Proc. Combust. Inst. 26 (1996) 43–48.
[17] J.A. Blasco, N. Fueyo, J.C. Larroya, C. Dopazo, J.Y. Chen, Single-step time-integrator of a methane-air chemical system using artificial neural networks, Comput. Chem. Eng. 23 (1999) 1127–1133.
[18] F. Flemming, A. Sadiki, J. Janicka, LES using artificial neural networks for chemistry representation, Prog. Comput. Fluid Dyn. 5 (2005) 375–385.
[19] A. Kempf, F. Flemming, J. Janicka, Investigation of lengthscales, scalar dissipation, and flame orientation in a piloted diffusion flame by LES, Proc. Combust. Inst. 30 (2005) 557–565.
[20] M. Ihme, C. Schmitt, H. Pitsch, Optimal artificial neural networks and tabulation methods for chemistry representation in LES of a bluff-body swirl-stabilized flame, Proc. Combust. Inst. 32 (2009) 1527–1535.
[21] B.A. Sen, S. Menon, Turbulent premixed flame modeling using artificial neural networks based chemical kinetics, Proc. Combust. Inst. 32 (2009) 1605–1611.

[22] M. Ihme, A.L. Marsden, H. Pitsch, Generation of optimal artificial neural networks using a pattern search algorithm: Application to approximation of chemical systems, Neural Comput. 20 (2008) 573–601.
[23] R.W. Bilger, S.H. Starner, R.J. Kee, On reduced mechanisms for methane-air combustion in nonpremixed flames, Combust. Flame 80 (1990) 135–149.
[24] A.W. Cook, J.J. Riley, G. Kosály, A Laminar flamelet approach to subgrid-scale chemistry in turbulent flows, Combust. Flame 109 (1997) 332–341.
[25] M.T. Hagan, H.B. Demuth, M.H. Beale, Neural Network Design, PWS Publishing, Boston, MA, 1996.
[26] S. Haykin, Neural Networks: A Comprehensive Foundation, Prentice Hall PTR, Upper Saddle River, NJ, 1994.
[27] A.E. Lutz, R.J. Kee, J.F. Grear, OPPDIF: A FORTRAN Program for Computing Opposed-flow Diffusion Flames, Sandia National Laboratories ReportSAND96-8243, 1996.
[28] G.P. Smith, D.M. Golden, M. Frenklach, N.W. Moriarty, B. Eiteneer, M. Goldenberg, C.T. Bowman, R.K. Hanson, S. Song, W.C. Gardiner Jr., V.V. Lissianski, Z. Qin. Available at: <http://www.me.berkeley.edu/gri_mech/>.
[29] F. Liu, H. Guo, G.J. Smallwood, Ö.L. Gülder, M.D. Matovic, A robust and accurate algorithm of the β-pdf integration and its application to turbulent methane–air diffusion combustion in a gas turbine combustor simulator, Int. J. Therm. Sci. 41 (2002) 763–772.
[30] W.P. Jones, B.E. Launder, The prediction of laminarization with a two-equation model of turbulence, Int. J. Heat Mass Transfer 15 (1972) 301–314.
[31] J.J. McGuirk, W. Rodi, The calculation of three-dimensional turbulent free jets, in: First Symposium on Turbulent Shear Flows, 1979, pp. 71–83.
[32] M.D. Emami, A. Kamranian, Application of the Hybrid method to numerical simulation of droplet evaporation and combustion, in: Proceedings of the International Conference on Recent Advances in Mechanical and Materials Engineering, Kuala Lumpur, May 2005.
[33] V. Bergmann, W. Meier, D. Wolff, W. Stricker, Application of spontaneous Raman and Rayleigh scattering and 2D LIF for the characterization of a turbulent CH_4 /H_2/N_2 jet diffusion flame, Appl. Phys. B 66 (1998) 489–502.
[34] E. Hassel, S. Geiß, 1998. Available at: <http://www.tu-darmstadt.de/fb/mb/ekt/flamebase.html>.
[35] <http://www.sandia.gov/TNF/DataArch/DLRflames.html>.
[36] W. Meier, R.S. Barlow, Y.-L. Chen, J.-Y. Chen, Raman/Rayleigh/LIF measurements in a turbulent CH_4 /H_2 /N_2 jet diffusion flame: Experimental techniques and turbulence–chemistry interaction, Combust. Flame 123 (2000) 326–343.
[37] M. Fairweather, R.M. Woolley, First-order conditional moment closure modeling of turbulent, nonpremixed methane flames, Combust. Flame 138 (2004) 3–19.
[38] H. Pitsch, Unsteady flamelet modeling of differential diffusion in turbulent jet diffusion flames, Combust. Flame 123 (2000) 358–374.
[39] F. Tabet, A. Boland, H. Mlaouah, B. Sarh, I. Gökalp, Investigation of turbulence models capability in predicting mixing in the near field region of hydrogen enriched natural gas turbulent non-premixed air flames, in: Fourth European Combustion Meeting, Vienna, Austria, 2009.
[40] R.J. Kee, F.M. Rupley, J.A. Miller, Chemkin II: A Fortran Chemical Kinetics Package for the Analysis of Gas-phase Chemical Kinetics, Sandia Report SAND89-8009, Sandia National Laboratories, Livermore, CA, 1989.